Crystallization of Poly(vinylidene fluoride)–Poly(methyl methacrylate) Blends: Analysis of the Molecular Parameters Controlling the Nature of the Poly(vinylidene fluoride) Crystalline Phase

C. Léonard, J. L. Halary,* and L. Monnerie

Laboratoire de Physicochimie Structurale et Macromoléculaire, Ecole Supérieure de Physique et de Chimie Industrielles de la Ville de Paris, 10, rue Vauquelin F-75231, Paris Cedex 05, France. *Received August 5, 1987; Revised Manuscript Received April 13, 1988*

ABSTRACT: The nature of the crystalline phase of PVDF in compatible blends with PMMA's of different tacticities was investigated by using a FT-IR technique. The β phase was observed after quenching from the melt and further annealing above the glass transition temperature over a composition range depending on PMMA tacticity. Two main factors were identified as controlling the nature of the crystalline phase: the nucleation temperature and the increase in tt conformations of PVDF due to specific interactions. It appears that the location of the glass transition temperature of the amorphous component is responsible for much of the crystallization behavior of PVDF.

Introduction

It is now well established that blends of PVDF and PMMA are compatible in the amorphous state in spite of their rather different solubility parameters, thermal coefficients of expansion, and isothermal compressibilities. The miscibility of the two polymers has been ascertained by various methods for probing the structure of the blends over characteristic lengths ranging from micrometers to angstroms.[1-8] A continuous change of the glass transition temperature with composition and a lowering of the PVDF melting point are observed.

As shown by FT-IR measurements, the major driving force for compatibility results from hydrogen bonding involving the carbonyl groups of PMMA and the CH_2 groups of PVDF.[9] The negative enthalpy of mixing stabilizes the mixture. However, the interactions between the two polymers are not strong enough to preclude partial crystallization of PVDF,[10] which leads to a lowering of the free energy of the mixture. Except at temperatures close to the melting point, the thermodynamically favorable state is characterized by PVDF crystals surrounded by an amorphous matrix where PVDF and PMMA are intimately mixed.

Pure PVDF can exist in a variety of crystal forms including α, β, γ and α_p. These forms and the variety of processes whereby they may be obtained and interconverted have been described by Lovinger.[11] As a general rule, the α form is obtained by crystallization from the melt.

We have shown in a previous study that the crystal phase of PVDF is very sensitive to blending with PMMA. The conformation of PVDF chains in the crystal phase depends on the composition and on the thermal history of the mixture. Blends containing around 70 wt % of PVDF may yield the piezoelectric β phase, provided the blend is quenched from the melt and then annealed above the glass transition temperature.[12]

This system may be further understood by varying the tacticity of PMMA. This offers an opportunity to produce blends with different T_g's and strengths of interaction. The difference in flexibility between the stereoisomers is reflected by the low glass transition temperature of isotactic PMMA (i-PMMA, T_g = 50 °C), compared to the high glass transition temperature of syndiotactic PMMA (s-PMMA, T_g = 115 °C). As a consequence, for blends of a given composition, PVDF/i-PMMA exhibits a lower glass transition temperature than PVDF/s-PMMA.

Table I
Triad Percentages of the Different PMMA Samples

sample	triad *mm*	triad *mr*	triad *rr*
a-PMMA	7%	38%	55%
i-PMMA	83%	12%	5%
s-PMMA	4%	23%	73%

The influence of PMMA tacticity on the energy of mixing has been investigated by Roerdink and Challa[13] through melting point depression measurements. The blend can be viewed as a solution, with PMMA acting as a good solvent. Because of the lower free energy in the mixed amorphous phase, the crystals of PVDF have a lower equilibrium melting point than pure PVDF. The melting point depression observation enables one to calculate the interaction coefficient. Although the melting point depression found by Roerdink an Challa is not entirely due to thermodynamic effects since the authors did not apply the Hoffman–Weeks analysis to correct for finite lamellar thickness and determine the equilibrium melting temperature, the interesting point of these results is that they permit a comparison of blends crystallized under the same conditions. Their results suggest stronger interaction of PVDF with isotactic than with atactic and syndiotactic PMMA.

The aim of the present work is to identify a set of parameters that, either individually or in combination, control the crystallization of PVDF in these blends. We shall focus on the influences of the crystallization temperature and of the specific interactions.

Experimental Section

Materials. PVDF, atactic PMMA (a-PMMA), and PVDF/a-PMMA blends were supplied by Solvay. They are the same as those used in previous studies.[9,12] Isotactic PMMA (i-PMMA) and syndiotactic PMMA (s-PMMA) were supplied by Polysciences. The copolymer poly(vinylidene fluoride–trifluoroethylene), P(VDF–TrFE), was obtained from Atochem. The tacticities of the different PMMA samples were checked by proton nuclear magnetic resonance (spectrometer Varian EM-390, 90 MHz; solvent, *o*-dichlorobenzene; temperature, 123 °C). Triad percentages are given in Table I.

Sample Preparation. Blends were cast from *N,N*-dimethylacetamide solutions onto potassium bromide pellets. The films were dried in a vacuum oven to remove the solvent completely; they were sufficiently thin to be within the absorbance range where the Beer–Lambert law is usually assumed to be obeyed (absorbance less than 0.8).

FT-IR Analysis. IR spectra were recorded on a Nicolet 7199 FT-IR spectrometer at 1- or 2-cm^{-1} resolution. From 100 to 1300

* To whom correspondence should be addressed.

0024-9297/88/2221-2988$01.50/0

interferograms were coadded and averaged, in order to improve the signal-to-noise ratio.

The relative amounts of α and β phases were determined according to the procedure developed by Osaki and Ishida.[14] The error bar may be estimated to be around 5%.

Self-Deconvolution of Spectra. Fourier self-deconvolution involves the deconvolution of a line-shape function from the experimental spectrum. The removal of the line shape reduces the bandwidth and thereby improves the "apparent" spectral resolution. Self-deconvolution software is routinely available on Nicolet FT-IR. The choice of the adjustable parameters in the computer program was the same as detailed in a previous publication,[9] i.e., 10 cm^{-1} for the half-bandwidth of the Lorentzian and 3 for the optimization parameter of the deconvoluted spectrum.

Factor Analysis. The general background of factor analysis (FA) has been reviewed by Koenig et al.[15] This method applies to systems of data in which a set of variables can be expressed as a linear combination of N factors. FA can be used for the determination of N.

In matrix notation, Beer's law is $\mathbf{A} = \mathbf{E} \cdot \mathbf{C}$. The dimensions of the absorbing matrix **A** are NW × NS where NW is the number of discrete wavelengths of digitized data and NS is the number of mixture spectra under study. **E** is the extinction coefficient matrix whose dimensions are NW × NC; NC is the number of linearly independent components in the mixture spectra. The dimensions of the concentration matrix **C** are NC × NS. Provided that NW > NC and NS > NC, the number of independent components NC is equal to the rank of **A**. Thus, calculation of NC reduces simply to finding the rank of the data matrix **A**.

A Nicolet program (PFANAL) calculates the covariance matrix of **A** and diagonalizes it. A set of eigenvalues and eigenvectors is obtained; the rank of **A** is given by the number of nonzero eigenvalues. In fact, none of the eigenvalues is strictly equal to zero, owing to the presence of random noise in experimental data. We have used the criterion of Antoon et al.[16] in order to distinguish nonzero and error eigenvalues: nonzero eigenvalues will be order(s) greater in magnitude than the error eigenvalues. The error eigenvalues will be of the same magnitude and clearly distinguished as a group.

X-ray Diffraction. X-rays were used to determine the overall degree of crystallinity of the specimens. Measurements were performed by using the ray Kα of copper (λ = 1.54 Å) and the ray Kα of molybdenum (λ = 0.71 Å). Diffraction spectra were first corrected for absorption and polarization effects and for Compton scattering and then deconvoluted in order to extract the amorphous and crystalline contributions. The error bar on the degrees of crystallinity is of about 5%.

Differential Scanning Calorimetry. The glass transition temperature and the melting endotherm of the various blends were recorded by using a Du Pont 1090 differential scanning calorimeter. The heating rate was 20 °C/min.

Results and Discussion

Nature of the Crystalline Form of PVDF. The PVDF/i-PMMA and PVDF/s-PMMA blends have been quenched from the melt and then annealed above T_g. From a qualitative viewpoint, the FT-IR spectra confirm that the α phase grows on both sides of the composition range, whereas the formation of the β phase is favored for intermediate compositions. However, a significant influence of PMMA tacticity on the crystallization of PVDF is observed. The concentration range within which PVDF can crystallize upon annealing is larger when i-PMMA is used (Figure 1). Moreover, the width of the composition window within which the β phase is evidenced depends on PMMA tacticity: it is broader for the system PVDF/i-PMMa than for PVDF/s-PMMA, which yields results roughly similar to those previously obtained with PVDF/a-PMMA.[12]

Crystallization results basically in the succession of two events: the primary nucleation of a new phase from the melt and then the three-dimensional growth of lamellae; these steps can be followed by lamellar thickening, fold surface smoothing, or reorganization into more perfect crystals.

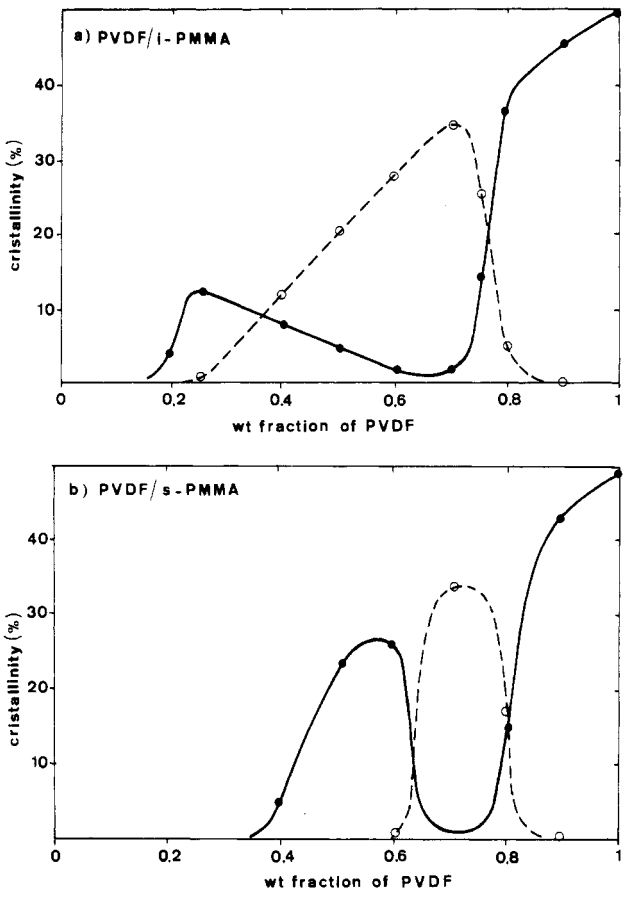

Figure 1. Degree of crystallinity versus PVDF weight fraction for the systems PVDF/i-PMMA (a) and PVDF/s-PMMA (b) after crystallization induced by annealing from the quenched state. (Solid and broken lines refer to the α phase and the β phase, respectively.)

First we shall focus on the rapid growth of the crystalline phase at the expense of the amorphous matrix. The following trends are characteristic of all the samples studied:

In PVDF/s-PMMA and PVDF/a-PMMA containing 50 wt % PVDF or more, and in PVDF/i-PMMA containing 30 wt % PVDF or more, about half the fraction of PVDF crystallizes, whatever the crystal form grown upon annealing. This corresponds to the situation encountered both in neat PVDF and in blends of PVDF/a-PMMA crystallized from the melt. Simultaneous crystallization of both the α and β forms (for example, in the PVDF/a-PMMA 60/40 blend) does not induce any increase in the overall crystallinity. The β phase develops at the expense of the α phase.

Except at high temperature where the β phase is unstable, no correlation holds between polymer structure and annealing temperature. In a given temperature range, α or (and) β can grow, depending on the initial composition of the blend. The above observations rule out the existence of two conformational populations having different requirements for crystallizing. However, this behavior is in contrast with that of isotactic polystyrene crystallized by exposure to specific solvent vapors. Tyrer et al.[17] have shown the existence of two conformational populations (the threefold helical and the extended conformations giving rise to the α and β phases, respectively), crystallizing under different conditions. When cocrystallization of both the α and β structures is achieved, a significant extra contribution of the β structure to the overall crystallinity is evidenced.

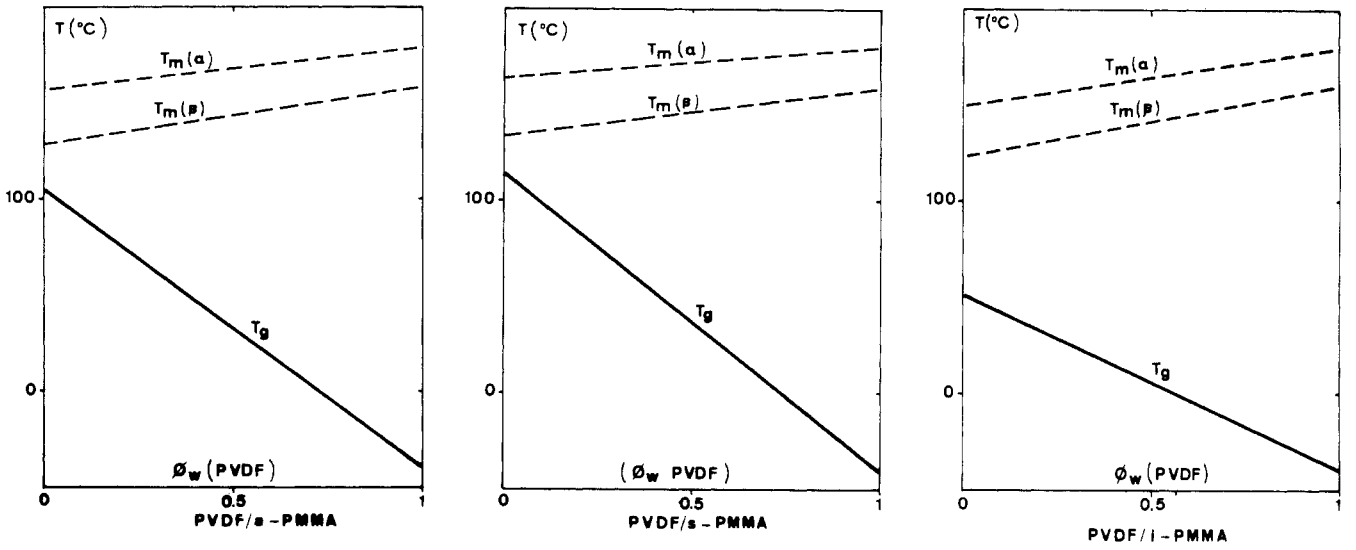

Figure 2. Sketch of crystallization domains of the systems PVDF/i-PMMA, PVDF/a-PMMA, and PVDF/s-PMMA.

The composition of the amorphous phase during the rapid growth of lamellae does not appear to be the main factor determining the nature of the PVDF phase. When PVDF crystallizes during annealing, the effective PMMA content in the residual melt increases without inducing any modification of the growing phase. The ratio of the growth rates of the two forms does not appear to be sensitive to the amorphous phase composition.

If the blend has already been nucleated during quenching from the melt, the crystal phase which develops upon further annealing has the same nature as the nuclei.

Theoretical Background. All these experimental findings suggest that the structure of the crystallizing polymer is likely to be determined by the nature of the nuclei. We shall therefore consider specifically the primary nucleation phenomenon.

A scheme to explain the kinetics of nucleation has been developed by Lauritzen and Hoffman.[18,19] A crystalline embryo consists of a parallel array of υ chain strands of length l and cross-sectional area a. Let us denote by σ_e and σ_s the end and side free energies of the nucleus and by Δf the free energy of melting of a boundless unit volume of crystal. The free energy of formation of a nucleus can be expressed as follows:

$$\Delta F(\upsilon,l) = -(la\upsilon)\Delta f + (2a\upsilon)\sigma_e + 2l(\upsilon a\pi)^{1/2}\sigma_s$$

The term $-(la\upsilon)\Delta f$ holds for the driving force for crystallization in the supercooled melt; the surface energy contribution, represented by the next two terms, is unfavorable and tends to destabilize the nucleus. For small l or υ values, the surface-to-volume ratio is small and the two latter terms dominate.

If the size of the nucleus is less than a critical one, given by l^* and υ^*, then the incorporation of a new strand induces an increase in the free energy. On the other hand, it is accompanied by a free energy lowering when the size exceeds l^* and υ^* and the nucleus grows spontaneously once the critical size is reached. The critical size is defined by

$$l^* = 4\sigma_e/\Delta f \quad \text{and} \quad \upsilon^* = 4\pi\sigma_s^2/a(\Delta f)^2$$

The free energy change upon formation of a critical nucleus is

$$\Delta F^*(\upsilon^*,l^*) = 8\upsilon\sigma_e\sigma_s^2/(\Delta f)^2$$

Finally, the nucleation rate, $\dot{N}$, varies as

$$\exp(-U/kT)\exp(-\Delta F^*/kT)$$

where U is the activation energy for the transport of strands to the nucleation site.

As a matter of fact, crystallization is confined in the temperature range between the melting point T_m and the glass transition T_g. The nucleation rate peaks at intermediate temperature. As schematized in Figure 2, blending may dramatically affect the temperature gap ($T_m - T_g$). Addition of PMMA greatly increases T_g and thus decreases the time the mixture spends between T_m and T_g during the step of cooling down from the melt. The rise in viscosity and the dilution of crystallizable units hinder molecular motions and delay the transport process of PVDF segments to the crystallite–melt interface. This tends to restrict the nucleation and growth process.

Interactions between PVDF and PMMA, which contribute to the free energy of mixing, further decrease the nucleation rate. By definition, the free energy of melting in the pure polymer is $\Delta f^0 = \mu m^0 - \mu c^0$ where μm^0 and μc^0 are the chemical potentials per mole of repeat units in the melt and in the crystalline state, respectively. In a blend, the free energy of melting Δf is given by Δf^0 plus an additional term due to the interactions between the two components:

$$\Delta f = \mu m - \mu c = (\mu m - \mu m^0) + (\mu m^0 - \mu c^0) = \Delta f^0 + (\mu m - \mu m^0)$$

$$\mu m - \mu m^0 = RT(V''/V')\chi\phi' = BV''\phi'^2$$

The superscripts $'$ and $''$ refer to as PMMA and PVDF and V, ϕ, χ, and B are the specific unit volumes, the volume fractions, the interaction parameter, and the interaction energy density, respectively.

Influence of the Temperature of Crystallization. For systems crystallizing upon cooling from the melt, addition of PMMA is shown to shift the crystallization exotherm to lower temperatures, which is consistent with a reduction of crystallization rate (Figure 3). PMMA enhances the supercooling effects upon quenching. In PMMA-rich blends, crystallization occurs so slowly that the glass transition can be reached before any appreciable crystallinity is developed: quenched samples are therefore amorphous. Experimental data demonstrate that the higher the T_g of the amorphous diluent, the more delayed the crystallization; quenching efficiency depends, for the major part, on the T_g of the mixture.

It may be suggested that the nucleation of the β phase is favored at low temperature. It has been shown by Hsu

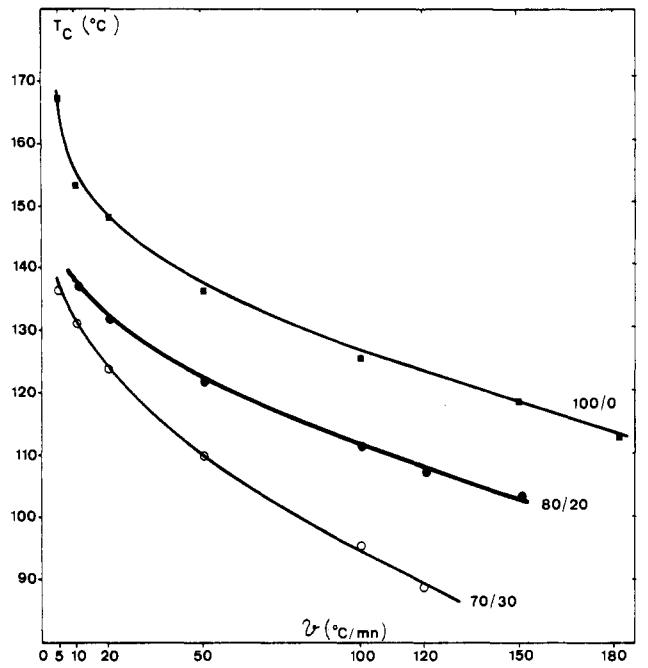

Figure 3. Crystallization temperature versus cooling rate for pure PVDF (■) and for blends PVDF/a-PMMA containing 80 (●) and 70 (○) wt % of PVDF.

and Geil[20] that suitable amorphization of neat PVDF at −160 °C allows further growth of the β crystal form at −30 °C. Such a behavior is unusual only because ultraquenching conditions cannot be satisfied on samples thicker than 100 nm. Similarly, the addition of PMMA favors the formation of the β phase because of the depression of the crystallization temperature. It seems likely that the ratio of the crystallization rates for the two phases is a function of temperature. At high and medium crystallization temperatures, only the α phase is formed owing to its significantly faster growth which renders it kinetically favored over the β phase (which is, in addition, unstable at high temperatures). There is the reversal of this trend in the case of very large supercooling, where the content of β nuclei increases.

This hypothesis is consistent with the occurrence of the α phase on both sides of the composition scale and of the β phase at intermediate compositions. In very rich PVDF blends, the crystallization is almost unaffected by the presence of PMMA because PVDF crystallizes from the melt at a high temperature where the α-phase nucleation rate is very fast. As more PMMA is added, the crystallization exotherm is drastically shifted and low nucleation temperatures are accessible upon quenching, owing to the low T_g of the mixtures. The nucleation rates of both phases are affected enough to permit matching between the α and β phases. In PMMA-rich blends, low nucleation temperatures are no longer accessible as a result of the high T_g of the mixtures. Annealing above T_g then gives rise to the α form.

Influence of PVDF–PMMA Interactions. Polymer–polymer interactions may also affect PVDF chain conformations. Specific interactions are very sensitive to the distance between the interacting groups and to their relative orientation: hydrogen bonding strength falls off rapidly when the atomic distance increases or when the bond is bent instead of linear. This infers that the efficiency of the contact between two unlike chains depends on their respective conformation (eventually tacticity) and flexibility. The chains are expected to adopt an optimate conformation for interacting. We have used molecular

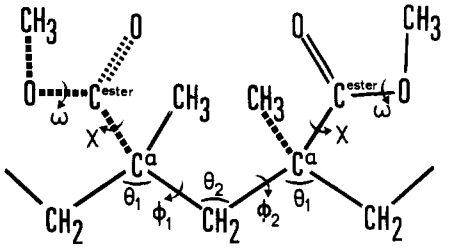

Figure 4. Representation of the angles defining the conformation of PMMA.

models in an attempt to investigate the dependence of the conformations of PVDF and PMMA chains on their association ability. In the amorphous state, PVDF exhibits short bond sequences tt and tg; the probability of a gg bond is negligible because of steric hindrance. The conformation of PMMA is defined by a set of rotation angles, as shown in Figure 4. Energy calculations emphasize that PMMA conformation remains close to all trans whatever the tacticity may be;[21] according to Flory, the probability of a trans bond is 0.72 for i-PMMA and 0.89 for s-PMMA. In the tt conformation the backbone torsion angles accord to the values $\phi = -20°$ for t− or $\phi = +10°$ for t+; the bond angles θ_1 and θ_2 are of around 106° and 124°, respectively. Finally, the ester group is approximately coplanar with the CH_3–C^{α}–C_{ester} bonds ($\omega = 0°$, $\chi = 0°$ or 180°). The isotactic conformation of lowest energy (t−t+t−t+) closely corresponds to a 10/1 helix, deviating only slightly from the extended-chain structure, identified in crystalline i-PMMA.[22] The conformation of lowest energy (t+t+t+t+) proposed for s-PMMA agrees well with wide-angle X-ray patterns.[23] The regular conformation persists over 16–20 backbone bonds. Because of unequal backbone bond angles, s-PMMA chains tend to form loops of long trans sequences, disrupted by gauche bonds. As for a-PMMA, it assumes predominantly syndiotactic sequences.

Let us assume, as a first, oversimplified analysis, that the PVDF chains adopt either the (tgtg′)n or the (tt)n regular conformations corresponding to the α and β phases, respectively. In addition, we will consider the PMMA chains as being in planar zigzag conformation and disregard small torsion angles and unequal backbone bond angles. Molecular models built with this assumption show unambiguously that the PVDF all-trans conformation allows more efficient interactions than the tgtg′ counterpart. This configuration greatly increases the probability for multiple interactions between two unlike chains. In the tt conformation, indeed, all the CH_2 groups have the same orientation with respect to the PVDF backbone. Furthermore, the spacing between the adjacent CH_2 groups nearly matches the spacing between the complementary carbonyl groups of PMMA. This infers that the occurrence of one hydrogen bond brings the adjacent CH_2 groups in the vicinity of carbonyl groups. These specific interactions, taking place over many units, may stabilize the regular conformation (tt)n. In contrast, the mismatch between the repeat distance characteristic of the PVDF chains in the tgtg′ conformation and the spacing between the ester groups are fairly large. This prevents every CH_2 group from interacting with every carbonyl group; some periodicity of interaction may occur only at long distance. It must be pointed out that the great persistence length of regular conformational sequences of PMMA may enhance the specific interactions. Chain stiffness also hinders deformations due to Brownian motion and thereby contributes to their stability; however, the length of sequences involved in the interactions is probably limited by the curvature of the backbone of a-PMMA or s-PMMA.

Table II
Results of Factor Analysis of the Spectra of Seven Mixtures of PVDF/a-PMMA Containing 15, 20, 25, 40, 45, 50, and 100 wt % of PVDF, Respectively

no.	λ	log λ	ind
1	95.326 47	1.97921	0.024 516
2	3.600 29	0.55634	0.018 532
3	1.010 13	0.00438	0.007 849
4	0.046 64	−1.3312	0.008 225
5	0.012 78	−1.89347	0.010 696
6	0.002 55	−2.59346	0.033 317
7	0.001 11	−2.95468	

Table III
Results of Factor Analysis of the Spectra of Eight Mixtures PVDF/a-PMMA, i.e., the Seven Ones Analyzed in Table I plus the Blend Containing 70 wt % of PVDF

no.	λ	log λ	ind
1	94.319 76	1.974 60	0.018 384
2	4.722 56	0.674 18	0.011 098
3	0.881 21	−0.054 92	0.004 958
4	0.046 40	−1.333 48	0.005 416
5	0.022 29	−1.651 89	0.005 647
6	0.005 44	−2.264 40	0.008 498
7	0.001 44	−2.841 64	0.029 496
8	0.000 87	−3.060 48	

Summing up, we may envision that (i) the interaction energy between the side surface of nuclei and the surrounding PMMA segments is lower for β than for α nuclei (NMR measurements[24] have shown that the amorphous region next to the growing crystals consists either of pure PMMA or of PMMA mixed with only a few PVDF chains) and (ii) PVDF all-trans sequences, induced by specific interactions, may act as nucleating sites for the β phase.

The equations giving l^*, v^*, and $\dot{N}$ as a function of the side surface free energy σ_s show that a decrease of σ_s is accompanied by a decrease of the critical size of nuclei and by an increase in the nucleation rate. If PMMA does not affect the surface free energy of α and β nuclei to the same extent, then the influence of PMMA on the nucleation will be quite different for the α phase and the β phase.

It is readily seen that the ratio $\dot{N}_\beta/\dot{N}_\alpha$ may be significantly increased only in mixtures crystallizing at low temperature; at low undercooling, indeed, the variation of σ_s is probably negligible compared to kT. This could further explain the growth of the β phase in an intermediate concentration range.

With the aim of checking the second assumption, we tried to gain some insight into the conformational structure of the molten blends. The first point is to know whether the spectra of the blends can be reproduced by coadding the spectra of the pure components. Factor analysis (FA), which allows one to determine the number of linearly independent components of a composite system, may provide the answer: if the trans/gauche ratio is different in neat PVDF and in PVDF mixed with PMMA, the spectra of the blends will be expressed as linear combinations of at least three components.

FA has been performed on two sets of PVDF/PMMA spectra in the conformation-sensitive region 930–1320 cm^{-1}; all the spectra were recorded in the molten state at 180 °C. The first set consisted of spectra of PVDF/a-PMMA mixtures with compositions giving rise exclusively to the α phase, namely, (in wt %) 15/85, 20/80, 25/75, 40/60, 45/55, 50/50, and 100/0. In the second set, the spectrum of the blend 70/30 was analyzed together with previous ones. Results relative to these two sets of spectra are given in Tables II and III, respectively: the eigenvalues λ are numbered in order of decreasing size. Plots of log λ versus eigenvalue number (Figure 5) allow nonzero and error

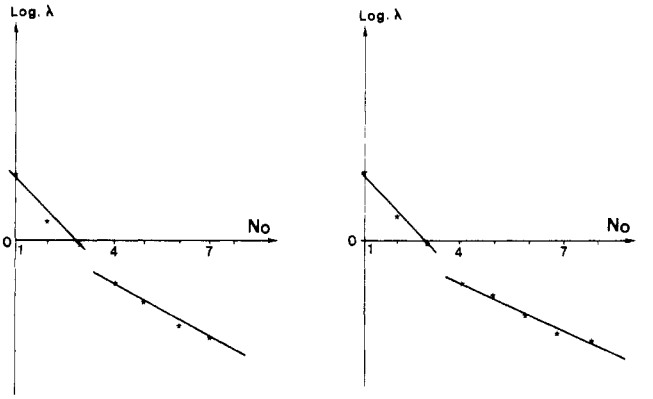

Figure 5. Analytical representation of FA results. Left diagram, data of Table II; right diagram, data of Table III.

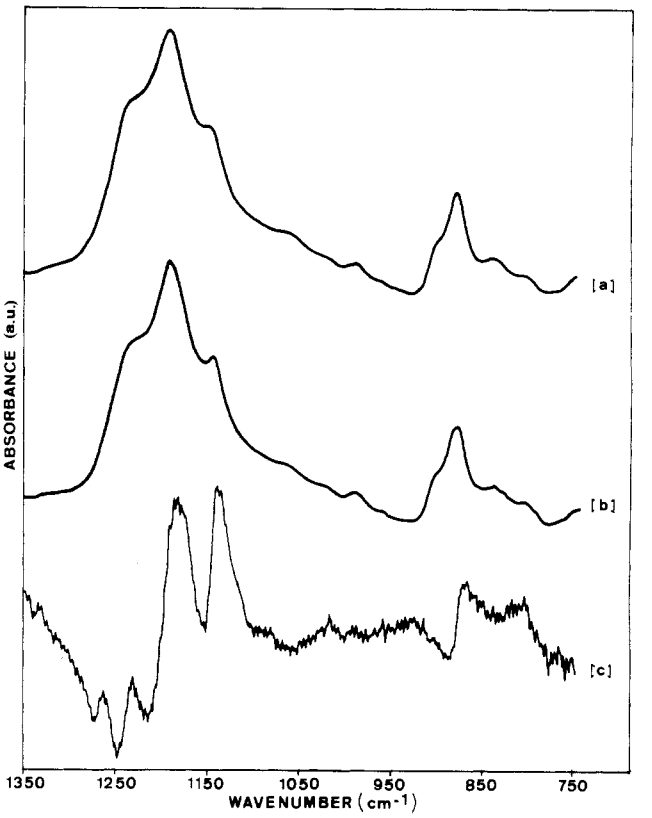

Figure 6. System PVDF/a-PMMA at 180 °C. (a) Experimental spectrum; (b) spectrum reconstructed by linear combination of neat component spectra; (c) difference spectrum (b) − (a).

eigenvalues to be distinguished according to Antoon's criterion[16] and indicate the presence of three linearly independent components in the spectra of both sets. The indicator function IND[25] reaches a minimum for $N_0 = 3$, in good agreement with these findings.

In an attempt to confirm the existence of the third component, we have substracted the spectra of the blends, reconstructed by linear combination of PVDF and PMMA spectra, from their experimental counterpart. An example is given in Figure 6. Bands in the difference spectrum are not easily assigned, due to the overlapping of PVDF and PMMA spectra. The first two components can be identified as PVDF and PMMA; the third could be due, at least partly, to PVDF conformational changes induced by interactions. Since FA of the second set, including the 70/30 spectrum, does not reveal the existence of any additional eigenvalue, this suggests that PVDF does not undergo a sudden conformational change in the 70/30 blend; it is probable that the conformational weights of trans and

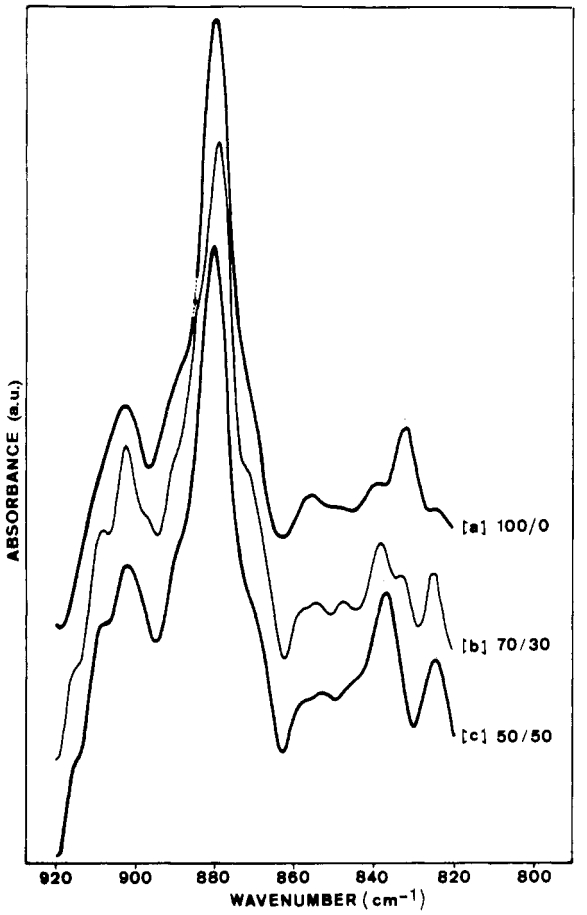

Figure 7. Self-deconvolution spectra of the system PVDF/a-PMMA. Weight percent of PVDF: (a) 100; (b) 70; (c) 30.

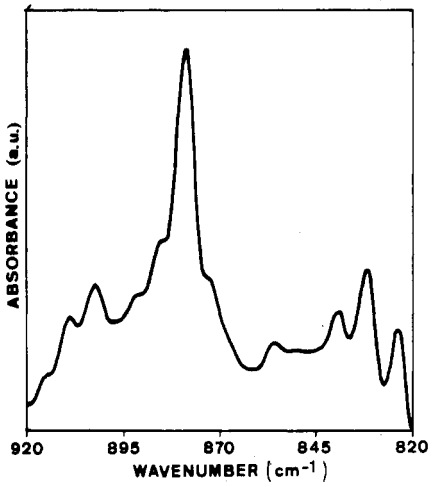

Figure 8. Example of self-deconvolution spectrum of the system PVDF/i-PMMA (blend containing 50 wt % of PVDF).

gauche conformations vary progressively as a function of composition.

Another spectral region permits a study of the increase in trans conformation weight: the band at 884 cm^{-1}, characteristic of short trans sequences, is evidenced in the blend PVDF/a-PMMA 70/30 by using the self-deconvolution method (Figure 7). It is no longer resolved for other compositions (for example 50/50) because the content of trans sequences is too small. On the other hand, in PVDF/i-PMMA blends, this band may be evidenced in a wider composition range, as shown in Figure 8 for the blend 50/50.

These results suggest that the statistical weight of trans sequences in the molten state increases upon adding

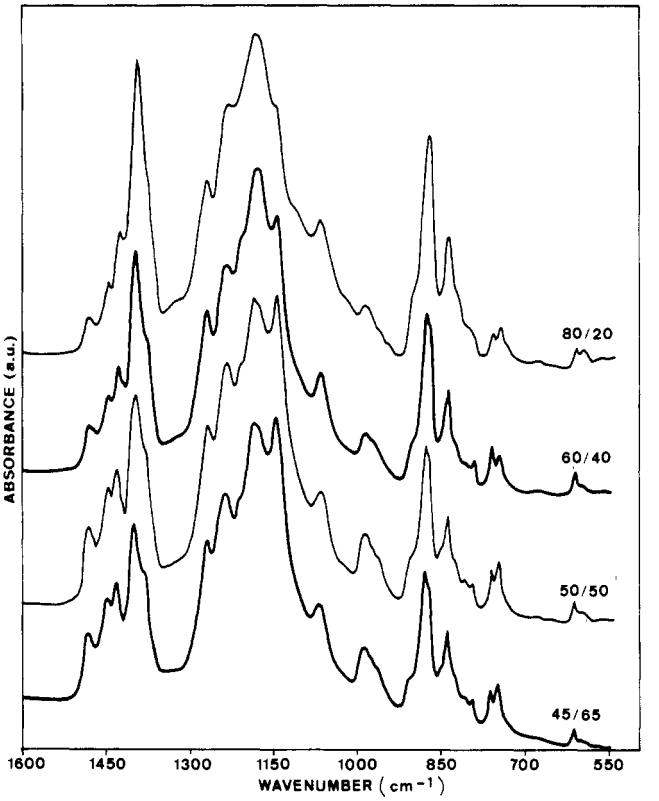

Figure 9. IR spectra of the system P(VDF–TrFE)/a-PMMA after crystallization induced by annealing. From top to bottom: 80, 60, 50, and 45 wt % of copolymer.

PMMA; moreover, the amplitude of the effect is a function of PMMA tacticity. Summarizing, one can infer that specific interactions are enhanced in the presence of all-trans conformations and that they lead to a favorable lowering of the enthalpy of mixing of the system. However, this decrease in energy is accompanied by an increase in the intramolecular energy of PVDF chains. As a consequence, the observed behavior is the result of a balance between these two effects.

Such a finding is supported by the study of blends of a-PMMA with a random copolymer of vinylidene fluoride and trifluoroethylene, P(VDF–TrFE), containing 5 mol % of TrFE units. In the neat state, this copolymer exhibits properties very similar to PVDF: same T_g; same crystallization temperature range; preferred formation of the α form. However, inclusion of TrFE units in the PVDF chains has the same qualitative effect that an increase in the amount of head-to-head defects in pure PVDF, namely, a lowering of the difference in intramolecular energies of the conformations tt and tgtg′. As a consequene for the crystallization of the blends, the β phase is observed over a wider composition range than with PVDF. As illustrated in Figure 9, the β phase is present in blends P(VDF–TrFE)/a-PMMA of composition 45/55 or 50/50, whereas we have shown it does not exist in blends PVDF/a-PMMA of the same composition.

Conclusion

Blending of PVDF with a compatible polymer such as PMMA permits control of the nature of its crystalline phase, provided suitable blend composition and thermal history are chosen. Thanks to the use of PMMA samples of different tacticity, it has become possible to determine the main factors governing the nature of the crystalline phase which is formed: (i) the temperature at which nucleation develops along the step of cooling from the melt and (ii) the intensity of specific interactions, the role of

which is to increase the tt content of PVDF chains.

This control of the PVDF crystalline phase upon blending is not peculiar to mixtures with PMMA. Indeed, we have recently observed a similar crystallization behavior of PVDF in blends with some other compatible polymers, characterized by different chemical structures.[26] These new data will be discussed in detail in a forthcoming publication.

Acknowledgment. We thank Drs. L. Bosio and C. Chassagnard for their kind and helpful assistance in the X-rays and NMR experiments, respectively. This work was supported by the "Centre National de la Recherche Scientifique" through Grant ATP 983004.

Registry No. PVDF, 24937-79-9; PMMA, 9011-14-7; i-PMMA, 25188-98-1; s-PMMA, 25188-97-0; (VDF)(TrFE) (copolymer), 28960-88-5.

References and Notes

(1) Noland, J. S.; Hsu, N. N. C.; Saxon, R.; Schmitt, J. M. *Adv. Chem. Ser.* **1971**, No. *99*, 15.
(2) Nishi, T.; Wang, T. T. *Macromolecules* **1975**, *8*, 909.
(3) Roerdink, E.; Challa, G. *Polymer* **1980**, *21*, 590.
(4) Hourston, O. J.; Hughes, I. D. *Polymer* **1977**, *18*, 1175.
(5) Coleman, M. M.; Zarian, J.; Varnell, D. F.; Painter, P. C. *J. Polym. Sci., Polym. Lett. Ed.* **1977**, *15*, 745.
(6) Wendorff, J. H. *J. Polym. Sci., Polym. Lett. Ed.* **1980**, *18*, 439.
(7) Douglass, D. C.; McBrierty, V. J. *Macromolecules* **1978**, *11*, 766.
(8) Lin, T. S.; Ward, T. C. *Polym. Prepr. (Am. Chem. Soc., Div. Polym. Chem.)* **1983**, *24*, 136.
(9) Lêonard, C.; Halary, J. L.; Monnerie, L. *Polymer* **1985**, *26*, 1507.
(10) Paul, D. R.; Barlow, J. W. In *Polymer Alloys II*; Klemper, D., Frisch, K. C., Eds.; Plenum: New York, 1980.
(11) Lovinger, A. J. In *Developments in Crystalline Polymers*; Bassett, D. C., Ed.; Applied Science: London, 1981.
(12) Lêonard, C.; Halary, J. L.; Monnerie, L.; Broussoux, D.; Servet, B.; Micheron, F. *Polym. Commun.* **1983**, *24*, 110.
(13) Roerdink, E.; Challa, G. *Polymer* **1978**, *19*, 173.
(14) Osaki, S.; Ishida, Y. *J. Polym. Sci., Polym. Phys. Ed.* **1975**, *13*, 1071.
(15) Gillette, P. C.; Lando, J. E.; Koenig, J. L. *Anal. Chem.* **1983**, *55*, 630.
(16) Antoon, M. K.; d'Esposito, L.; Koenig, J. L. *Appl. Spectrosc.* **1979**, *33*, 349.
(17) Tyrer, N. J.; Bluhm, T. L.; Sundarajan, P. R. *Macromolecules* **1984**, *17*, 2296.
(18) Lauritzen, J. I.; Hoffman, J. D. *J. Res. Natl. Bur. Stand. (U.S.)* **1960**, *64*, 73.
(19) Hoffman, J. D.; Lauritzen, J. I. *J. Res. Natl. Bur. Stand. (U.S.)* **1961**, *65*, 297.
(20) Hsu, C. C.; Geil, P. H. *J. Appl. Phys.* **1984**, *56*, 2404.
(21) Sundarajan, P. R.; Flory, P. J. *J. Am. Chem. Soc.* **1974**, *96*, 5025.
(22) Tadokoro, H.; Chatani, Y.; Kusanagi, H.; Yokoyama, M. *Macromolecules* **1970**, *3*, 441.
(23) Lovell, R.; Windle, A. H. *Polymer* **1981**, *22*, 175.
(24) Tekely, P.; Lauprêtre, F.; Monnerie, L. *Polymer* **1985**, *26*, 1081.
(25) Malinowski, E. A. *Anal. Chem.* **1977**, *49*, 606.
(26) Lêonard, C.; Halary, J. L.; Monnerie, L. "On the Nature of the Crystalline Phase of PVDF in Blends with Compatible Amorphous Polymers". Presented at the European Symposium on Polymer Blends, Strasbourg, France, May 25–27, 1987.

Crystallization of Randomly Epoxidized *trans*-1,4-Polyisoprene

Jia-rui Xu and Arthur E. Woodward*

Chemistry Department, The City College and the Graduate School, The City University of New York, New York, New York 10031. *Received December 10, 1987*

ABSTRACT: Copolymers of *trans*-1,4-polyisoprene containing from 1 to 10% randomly placed epoxidized units were crystallized from solution. The crystal form from infrared spectroscopy, the DSC melting endotherm(s), and the reacted and unreacted block lengths, as obtained by surface epoxidation in suspension followed by carbon-13 solution NMR, were determined. Small amounts of oxirane units (1–2%) have no significant effect on the melting endotherm or block lengths but do change the crystal form and the redissolution temperature. Evidence for incorporation of oxirane units in the crystal core is discussed.

Introduction

The quantitative characterization of single lamellas and lamellar structures of *trans*-1,4-polybutadiene, TPBD, and *trans*-1,4-polyisoprene, TPI, has been carried out by using a surface reaction coupled with carbon-13 solution nuclear magnetic resonance measurements.[1-6] This procedure yields the fraction reacted and the average reacted and unreacted block lengths of the modified chains. For single lamellas at moderate to high molecular weight and with the proper choice of reaction conditions these parameters can be equated to the total surface fraction, the average fold length and the crystalline stem length, respectively. For multilamellar structures the reacted block length is equated to an average noncrystalline chain traverse length, characteristic of the folds and any interlamellar traverses present.

The effects of polymer molecular weight (M_v = 7000–36 000) and of crystallization solvent and temperature on the morphology, the crystallinity, the surface fraction, the crystalline stem length, and the average reacted block length have been studied for 99% trans-, 1% cis-1,4-polybutadiene crystallized from dilute solution.[2] The average reacted block length increased from 5 to 9 with a change in crystalline stem length from 15 to 24 but with the crystallinity remaining at 0.24–0.27; it was also found that within the detection limits the cis units present in the chains appear at the lamellar surfaces and that the measured parameters were independent of crystallization concentration up to 5%. Lamellas of a 88.5% trans-1,4-, 10% cis-1,4-, 1.5% 1,2-polybutadiene with $M_w = 4.6 \times 10^5$ were obtained from solution by using various crystallization conditions with gels being formed above a concentration of 0.7%.[3] All of the crystalline products from this sample gave an average reacted block length of 11 ± 1 and a crystalline stem length of 16 ± 1. It was also determined that about 5% of the cis units was incorporated in the crystal core and the remainder excluded and appearing at the lamellar surfaces.

TPI fractions, containing no detectable amounts of the other isomeric units, with molecular weights (M_v) of 0.5×10^5 to 7×10^5 were crystallized from solution by using conditions that individually give single β-form lamellas,

0024-9297/88/2221-2994$01.50/0